Materials Letters, Volume 252, October 2019, pp. 211-214
DOI: 10.1016/j.matlet.2019.05.131

2D ultrathin carbon nanosheet derived from interconnected Al-MOF as excellent hose to anchor selenium for Li-Se battery

Wen-wu.Jin [a] , He-Jun. Li [a] , Ji-zhao Zou [b,], Saikumar Inguva [b], Qi Zhang[c], Shao-zhong Zeng [b], Guo-zhong Xu [b] , Xie-rong Zeng [b*]*

a. State Key Laboratory of Solidification Processing, Carbon/Carbon Composites Research Center, Northwestern Polytechnical University, Xi'an 710072, China

b. Shenzhen Key Laboratory of Special Functional Materials & Shenzhen Engineering Laboratory for Advance Technology of Ceramics, College of Materials Science and Engineering, Shenzhen University, Shenzhen 518060, PR China

c. School of Aerospace, Transport and Manufacturing, Cranfield University, Cranfield, Bedfordshire MK43 0AL, UK

*** Correspondence: zoujizhao@szu.edu.cn (J Z.Zou); zengxier@szu.edu.cn (X R.Zeng)**

ABSTRACT

Alleviating volume expansion of electrodes and improving utilization of the active materials have become key problems restricting a successful commercialization of lithium−selenium batteries. In this paper, a 2D ultrathin carbon nanosheets derived from interconnected MOF is designed for the first time. Such carbon nanosheets are composed by parallel stacked 2D sub-units, and this unique hierarchical porous architecture is beneficial for buffering the volume expansion and for improving the utilization rate of active materials. Therefore, the cathode displays an excellent cycling stability with a reversible capacity of 347.3 mAh g^{-1} at 2C after 240 cycles.

Introduction

The rapid development of portable electronic devices together with electrically powered vehicles urgently need alternative batteries featuring high energy density and excellent cycling stability. In this

regard, lithium-selenium (Li-Se) batteries have received a great attention in recent years, and these are regards as a competitive alternative to the Li-S batteries [1, 2]. However, the Li-Se battery system also suffers from a shuttles effect. In order to improve electrochemical performance of the Li-Se battery, researchers try to inhibit the shuttle effect by preparing carbon/selenium composite materials [3-6]. This is because carbon with hierarchical porous structure not only improve the conductivity of the electrode materials but also restrain the dissolution of the lithium polyselenides [3]. Therefore, a large number of carbon with special topological structures have been prepared [4-6].

Metal-organic framework (MOF) derived carbon has large specific surface area, abundant topological structures, and adjustable pore size, which can load Se effectively. Therefore, the MOF-derived carbon structures have been widely used in the Li-Se battery [3-5, 7]. Meanwhile, the appearance of self-assembled MOF materials is greatly expands the application of MOF, those superstructures inherit the exceptional properties of the MOF, and acquire certain unconventional advantages [8]. To the best of our knowledge, there has been no report on the preparation of electrode materials using self-assembled MOF as precursor in the field of Li-Se batteries.

In this study, the self-assembled Al-MOF (SAM) was obtained by an in-situ self-assembly strategy. After further carbonization and acid treatment, the ultrathin carbon nanosheets (UCNS) with large specific surface area and hierarchical porous structure were prepared. The UCNS-Se composite displays superior comprehensive battery properties, and these encouraging results suggests that the electrode materials prepared using SAM is good candidates in energy storage.

2. Experimental

For the synthesis of SAM: 4,4'-Bibenzoic acid (0.0651g) and $Al(NO_3)_3.9H_2O$ (0.1401g) were added in 10 mL of N,N-dimehylformamide. After stirring it for 30 min at room temperature, the mixture was added to a 15 ml, teflon-lined autoclave and kept it at 120 °C for 24 h. After that, the SAM was obtained by centrifugal separation, ethanol cleaning and drying at 80 ºC, respectively. In order to prepare UCNS, the SAM was annealed at 800 ºC for 1 h, and the as-prepared carbonized sample was then immersed in dilute

hydrochloric acid (10%). After sealing treatment, the sample was stored at 80 ºC. The UCNS-Se composites were prepared using UCNS (0.10g) and Se (0.25 g, Sigma Aldrich, 99.9%), and this mixture was then heated at 260 ºC for 20 h.

Scanning electron microscopy (SEM) and energy dispersive spectroscopy (EDS) were carried out using a field emission SU-70 microscopy. TEM images were collected using a JEOL JEM2010 electron microscope. The phase composition was tested using X-ray Diffractometer (XRD). A thermo-gravimetric analysis (TGA) was employed to observe the thermal stability of the SAM under nitrogen atmosphere. Raman, Brunauer-Emmett-Teller (BET, ASAP 2020 system), Elemental analysis (Elementar) and X-ray photoelectron spectroscopy (XPS) were also used to study the physical and chemical properties of the UCNS and UCNS-Se.

Electrochemical properties were measured using CR2032 coin-type cells. Electrodes were prepared by coating a mixture of the UCNS-Se with carbon black and sodium alginate in the ratio of 8:1:1 onto an aluminium foil, respectively. Thereafter, coin-cells were fabricated in an argon-filled glove box (Vigor Glove-boxes) and charged/discharged using a Neware battery testing system. Electrochemical impedance spectroscopy (EIS) and cyclic voltammetry (CV) measurements were performed using a CHI660D electrochemical workstation.

3. Results and discussion

The powder XRD of SAM is shown in Fig. 1.(a), which agrees well with the XRD diffraction peaks simulated by Senkovska et al. [9] The peak broadening phenomenon was observed, and it is attributed mainly to the effect of the small crystal sizes [9,10]. As shown in Fig. 1.(b, c), the SAM has a thin-sheet morphology with an average grain diameter is about 210 nm (Fig. S1).

According to the TGA curve (Fig. 1.(d)), weight loss of the SAM is about 18% in a temperature range 40–400 °C, and this process corresponds to the removal of guest molecules and water. The weight loss was increased sharply after 430 °C and this increase was continued until 610 °C. The final residual solids were accounted for 32.3% of the total initial mass.

As shown in Fig. 2(a, b), the UCNS retain the structure of the SAM. The low-magnification TEM (Fig. 2(d,

e)) shows that the lamellar structure is composed by interconnected 2D sub-units, while a high-magnification TEM (Fig. 2(f)) shows that size of the 2D sub-unit are about 30 nm. As shown in Table 1, the UCNS have a relatively higher carbon-oxygen ratio, which may lead to improve conductivity of the electrode [11]. The UCNS have a hierarchical porous structure. (Fig. 2(c)) [12]. The measured BET and pore volume are 1449.2 m^2/g and 1.74 cm^3/g, respectively.

The UCNS-Se was prepared by a melt-infiltration method. As shown in Fig. S2(f), the weight loss is about 64% for the UCNS-Se. After Se loading, there was no agglomeration of Se on the surface of the UCNS-Se (Fig. S3), which indicates that the Se was successfully anchored by the pore structure.

The Raman peak of the UCNS-Se (Fig. 2(g)) is similar to the characteristic peak of carbon (1350 and 1592 cm^{-1}) while a weaker peak was observed at 236 cm^{-1}, which indicates that Se is successfully loaded into the UCNS [7]. The XRD characteristic peaks are illustrated in Fig. 2(h). After impregnation of Se into the UCNS, the XRD peaks of the Se were disappeared. This phenomenon means that the amorphous Se was confined within the porous carbon [3, 12]. The XPS survey spectra of the UCNS-Se are shown in Fig. 2(i), the characteristic peak of C (284.5 eV), O (531 eV) and Se3d (55 eV) were observed, which confirms the existence of C, O and Se elements in the UCNS-Se. The Se 3d characteristic peak (55 eV) was divided into two peaks as shown in Fig. 2(i), which agrees fairly well with previous report [13].

The electrochemical performance of the UCNS-Se is shown in Fig. 3. The rate capability of the UCNS-Se is shown in Table S1 and Fig. 3(a). After the rate test, the original capacity of the UCNS-Se was largely recovered, which indicates that the UCNS–Se electrode is highly stable. The cycle performance of the UCNS–Se was evaluated at 2 C, as shown in Fig. 3(b), and the UCNS–Se electrode displays an excellent cycling stability with a reversible capacity of 347.3 mAh g^{-1} even after 240 cycles. This excellent electrochemical performance is attributed to the special nanostructure of the UCNS. The architecture is beneficial for buffering volume expansion that caused by Se transformation. It can be further validated by Fig. S5 that there is no obvious cracking or suffering pulverization in the electrode, except a slight volume expansion after 240 cycles at 2 C. Additionally, an improvement of the conductivity of the UCNS-Se can be confirmed by EIS analysis (Fig. 3(c)). The CV test was used to reveal redox mechanism of the Li-Se battery, as shown in Fig. 3(d). During the first cycle, the CV curve

displays two anode peaks (1.86 V and 2.17 V), which are due to the side effects and oxidation of the Se in the activation process of the cathode [14]. On the other hand, three cathode peaks at 1.94, 1.62 and 1.40 V were also observed, which can be attributed to the conversion of Se to Li_2Se [14].

4. Conclusion

In this study, the interconnected MOF-derived 2D carbon nanostructures were designed for the first time, and this method does not require of any template and carbon activation process. Additionally, the synthesis route reported in this work is an environment-friendly, cost-effective and easily industrialized method. This unique architecture is beneficial for buffering volume expansion that caused by Se transformation, and for improving the utilization rate of active materials. The UCNS–Se electrode displays an excellent cycling stability with a reversible capacity of 347.3 mAh g^{-1} at 2 C even after 240 cycles.

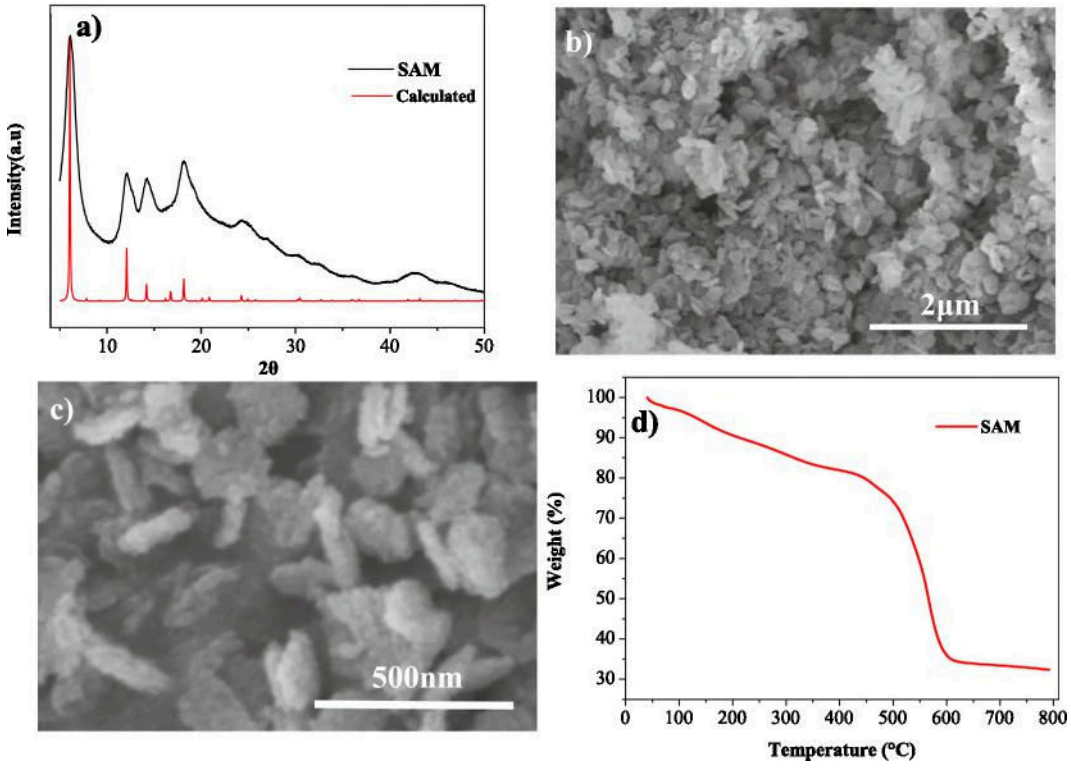

Fig. 1. a) X-ray diffraction patterns of calculated Al-MOF and SAM; (b, c) SEM images of the SAM; d) TGA curves of the SAM.

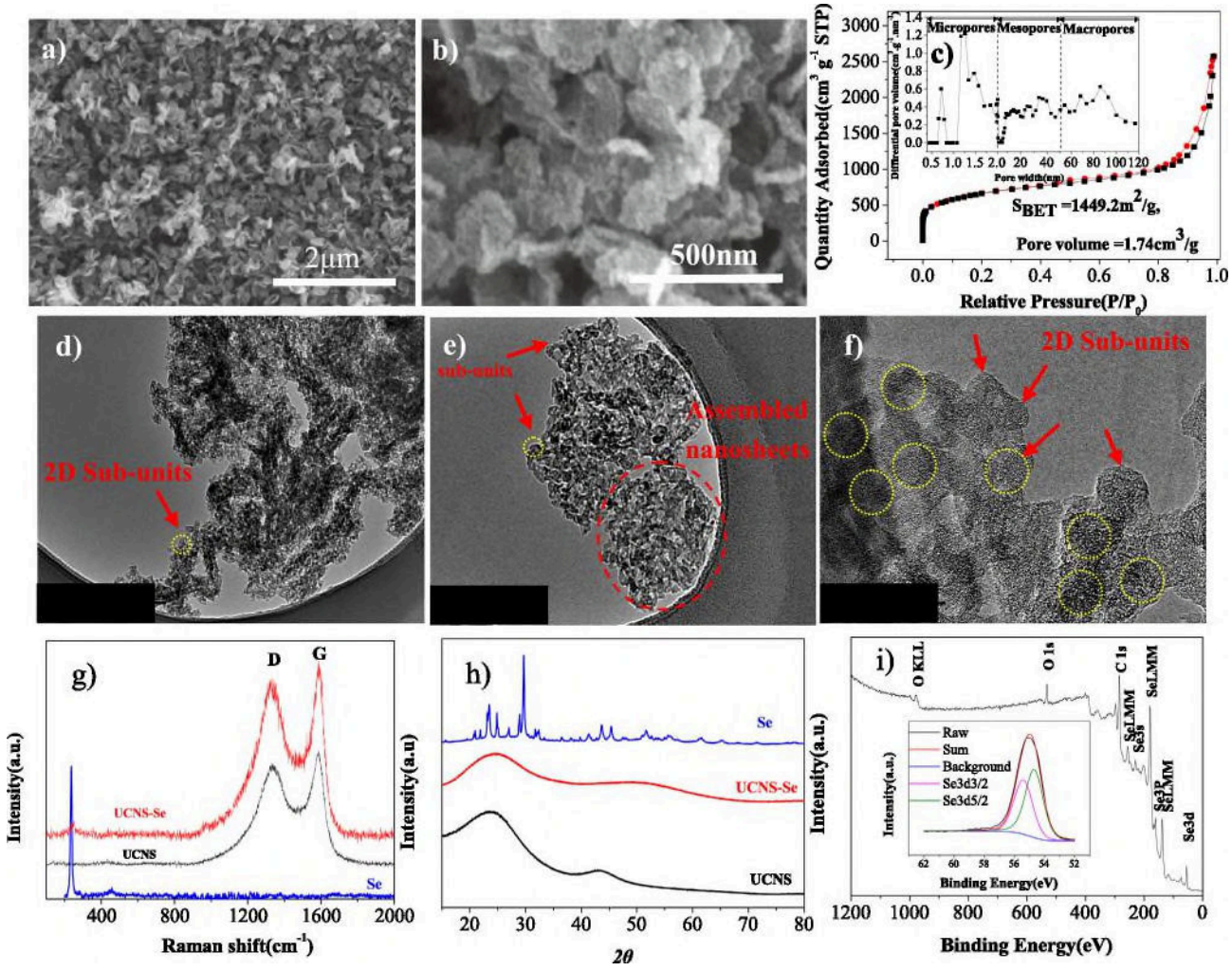

Fig. 2. (a, b) SEM images of UCNS with different magnifications; (c) BET and pore size distribution of the UCNS using DFT analysis; (d, e) Low- and (f) high-magnification of TEM images for the UCNS; (g) Raman and (h) XRD patterns of the pure Se, pure UCNS and UCNS-Se; (i) XPS survey spectrum and Se 3d XPS spectra of the UCNS-Se.

Table 1Elemental Analysis Results for the UCNS.

Samples ratio	N [wt%]	C [wt%]	H [wt%]	S[wt%]	O [wt%][a]	C/O
UCNS (800)	0.02	88.3	0.579	0.086	11.015	8.016

[a] The oxygen contents were calculated by subtracting other components from 100%.

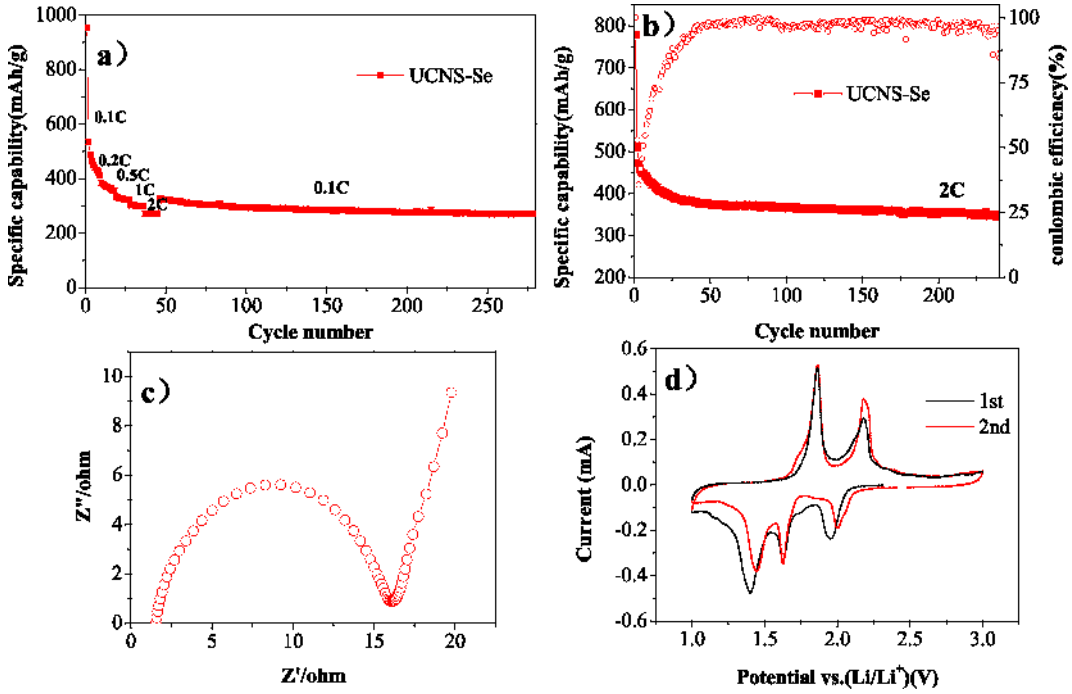

Fig. 3. (a) Rate performances of the UCNS–Se; (b) Cycle performance of the UCNS–Se cathodes at 0.5 C; (c) The equivalent circuit for the battery; (d) CV curve of the UCNS–Se.

Acknowledgements

This work was financially supported by the National Natural Science Foundation of China (Nos. 51202150 and 51272161), foundation of the State Key Laboratory of Solidification Processing in NWPU (SKLSP201110) and Shenzhen Basic Research Program (No. JCYJ20160422091418366).

References

[1] A. Eftekhari, Sustain. Energy Fuels 1 (2017) 14–29.

[2] J. Jin, X.-C. Tian, N. Srikanth, L.-B. Kongc, K. Zhou, J. Mater. Chem. A 5 (2017) 10110–10126.

[3] Y.-Q. Lai, Y.-Q. Gan, Z.-A. Zhang, W. Chen, J. Li, Electrochim. Acta 146 (2014) 134–141.

[4] T. Liu, M. Jia, Y. Zhang, J. Han, Y. Li, S.-J. Bao, D.-Y. Liu, J. Jiang, M.-W. Xu, J. Power Sources 341 (2017) 53–59.

[5] T. Liu, C.-L. Dai, M. Jia, D.-Y. Liu, S.-J. Bao, J. Jiang, M.-W. Xu, C. Ming, ACS Appl. Mater. Interfaces 8 (2016) 16063–16070.

[6] K. Balakumar, N. Kalaiselvi, Carbon 112 (2017) 79–90.

[7] Z.-Q. Li, L.-W. Yin, Nanoscale 7 (2015) 9597–9606.

[8] C.-S. Arnau, I. Inhar, K. Stylianou, D. Maspoch, Chem. Eur. J. 20 (2014) 5192– 5201.

[9] I. Senkovska, F. Hoffmann, M. Froba, J. Getzschmann, W. Bohlmann, S. Kaskel, Microporous Mesoporous Mater. 122 (2009) 93–98.

[10] J. Ellis, Z.-D. Zeng, S. Hwang, S.-B. Li, T.-Y. Luo, S. Burkert, D. White, N. Rosi, J. Gassensmith, A. Star, Chem. Sci. 10 (2019) 737–742.

[11] C. Punckt, F. Muckel, S. Wolff, I. Aksay, C. Chavarin, G. Bacher, W. Mertin, Appl. Phys. Lett. 102 (2013) 023114.

[12] J.-J. Zhou, J. Yang, Z.-X. Xu, T. Zhang, Z.-Y. Chen, J.-L. Wang, J. Mater. Chem. A 5 (2017) 9350–9357.

[13] K. Han, Z. Liu, J.-M. Shen, Y.-Y. Lin, F. Dai, H.-Q. Ye, Adv. Funct. Mater. 25 (2015) 455–463.

[14] Z.-Q. Yi, L.-X. Yuan, D. Sun, Z. Li, C. Wu, W.-J. Yang, Y.-W. Wen, B. Shan, Y.-H. Huang, J. Mater. Chem. A 3 (2015) 3059–3065.

2019-05-29

2D ultrathin carbon nanosheets derived from interconnected Al-MOF as excellent hosts to anchor selenium for Li-Se battery

Jin, Wen-Wu

Elsevier

Jin WW, Li HJ, Zou JZ, et al., (2019) 2D ultrathin carbon nanosheets derived from interconnected Al-MOF as excellent hosts to anchor selenium for Li-Se battery. Materials Letters, Volume 252, October 2019, pp. 211-214

https://doi.org/10.1016/j.matlet.2019.05.131